RSC Advances

This article can be cited before page numbers have been issued, to do this please use: S. Kanaparthi and S. Badhulika, *RSC Adv.*, 2016, DOI: 10.1039/C6RA21457F.

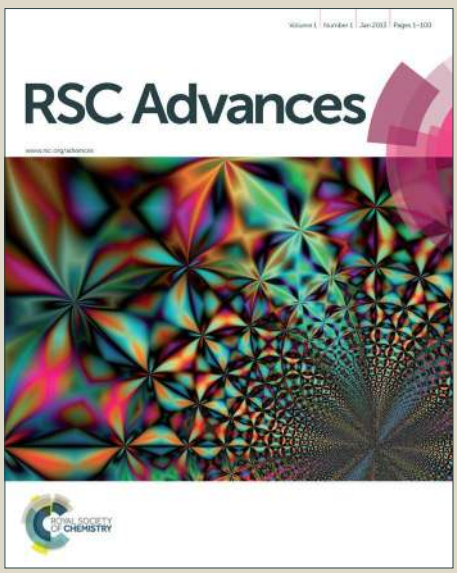

ROYAL SOCIETY OF CHEMISTRY

www.rsc.org/advances

View Article Online
DOI: 10.1039/C6RA21457F

Solvent-free fabrication of paper based all-carbon disposable multifunctional sensors and passive electronic circuits

Srinivasulu Kanaparthi and Sushmee Badhulika*

Department of Electrical Engineering, Indian Institute of Technology Hyderabad, Kandi, 502285, India.

*Corresponding Author: Email: sbadh@iith.ac.in

Abstract

In light of recent interest in green fabrication of electronics, we report eco-friendly engineered temperature sensor, pH sensor, humidity sensor and passive Resistor-Capacitor (RC) filters by solvent-free processing of graphite on cellulose paper. This was achieved via direct writing of graphite pencil on cellulose paper which involves the deposition of few layers to multi layers of conductive graphene flakes intercalated by clay and wax. The temperature sensor exhibits a negative temperature coefficient of resistance of -4232 ppm/K, which is comparable to that of conventional temperature sensors (Platinum, Nickel, and Copper) that are fabricated by capital intensive and complex procedures. The dynamic response of the temperature sensor shows its repeatability with excellent response time of 13.5 sec. The all-carbon pH sensor could efficiently distinguish acidic, alkaline and neutral solutions with significant sensitivity from 1.77 kΩ/pH to 2.21 kΩ/pH. The higher sensitivity of the pH sensor is attributed to the oxygen functional groups present in pencil graphite which undergoes protonation and deprotonation in presence of H^+ and OH^- ions to alter the conductivity of graphite trace. The interdigitated capacitive humidity sensor shows a linear response to humidity with fast response (1.5-2 sec) and recovery times (6-7 sec). These fast response and recovery times are due to fast adsorption and evaporation kinetics of water molecules on polar OH groups of cellulose fibers in paper, which depends on porosity of the paper. The versatility of the pencil-on-paper approach was further explored by drawing resistor and interdigitated capacitor in series to fabricate in-plane all-carbon RC filter which

View Article Online
DOI: 10.1039/C6RA21457F

demonstrate anticipated functionality with a cut-off frequency of 6 kHz. To the best of our knowledge, no studies have been reported on direct-write graphite on paper based in-plane all carbon passive electronic circuits, pH sensor and humidity sensor. This cleanroom-free approach further expands the scope of graphite on paper as a functional material in developing sensors and circuits for greener consumer electronics thereby causing no environmental contamination either in their production or disposal.

Keywords

Paper electronics, pH sensor, Humidity Sensor, Temperature sensor, Solvent-free fabrication.

1. Introduction

The fabrication of electronic devices on paper is considered as a promising solution for the realization of inexpensive, eco-friendly, use-and-throw disposable electronics [1, 2]. So far several efforts have been made to realize paper electronics including technologies such as lithography and physical/chemical vapor deposition. Even though these methods are highly efficient and progressive, complexity and expensive process steps make them unsuitable for small scale production. Alternatively, printing techniques have been studied and implemented to realize efficient and robust electronic devices like gas sensors [3], biosensors [4], transistors [5], energy storage devices [6] and touchpad [7]. However, the synthesis of conductive inks used in printing involve eco-unfriendly volatile organic solvents, surfactants, stirring or sonication for dispersion of nanomaterials and deposition of these conductive inks require plasma treatment of substrates which are complex and time consuming. All these pre-fabrication and post-fabrication multi step processes make it expensive, complicated and eco-unfriendly. In addition, there is a possibility that the structure and functionality may change when the nanomaterial is mixed in an organic solvent and thus efficiency of the device may be affected.

View Article Online
DOI: 10.1039/C6RA21457F

In order to address the aforementioned issues, a solvent-free fabrication of chemical and physical sensors have been reported with binder free Carbon Nanotube (CNT) composite pencils or pellets [8, 9]. Despite being efficient and solvent-free method, the cost of the CNT makes it rather expensive and the binder free CNT pellet is not strong enough to write sensors, components and circuits on paper with precise control. Alternatively, commercially available graphite pencil on paper has emerged as a material in implementing low cost, flexible, biodegradable electronics in use-and-throw applications. Owing to its outstanding electrical, mechanical and chemical properties, graphite was demonstrated as an active material in devices such as transistors [10, 13], circuits [10, 11], energy storage devices [12], strain sensors [13, 16], thermal flow sensors [14] and electrochemical sensors [15]. The fruitful implementation of these devices without using any toxic and expensive materials reveals that there is a lot of scope to develop other inexpensive and eco-friendly devices utilizing this methodology.

In this work, we report the fabrication of physical and chemical sensors by direct writing of pencil graphite on paper (GoP) which is an inexpensive and eco-friendly method. The HB pencil graphite trace on paper was utilized as a temperature and pH sensors. The temperature sensor exhibited excellent temperature coefficient of resistance (TCR) (The rate of change of normalized resistance per degree Celsius of temperature) which attributed to the presence of defects in the HB pencil graphite. The pH sensor was able to distinguish real time samples over a wide pH range as diverse as lemon juice, DI water and detergent solution with significant sensitivity and reproducibility. The 5B pencil graphite interdigitated capacitor on cellulose paper was demonstrated as a humidity sensor. The sensor exhibited excellent sensitivity towards exhaled breath and hot water vapor. The response and recovery times are very high, which are attributed to the fast adsorption and de-adsorption of water molecules on cellulose fibers. The fast adsorption and de-adsorption of moisture on paper are due to

View Article Online
DOI: 10.1039/C6RA21457F

capillary pressure and spreading of water molecule on paper respectively. The versatility of the GoP was further extended to realize passive electronic circuits which act as the basic backbone of most modern day electronic devices. The RC (Resistor-Capacitor) filter was fabricated by drawing a trace which acts as a resistor in series with interdigitated capacitor. As fabricated RC circuit has been demonstrated as an integrator (low pass filter) and a differentiator (high pass filter) and it exhibited a cut-off frequency of 6 kHz. The successful fabrication of low cost and eco-friendly passive RC filters on paper indicates that this approach can be utilized widely in use-and-throw and disposable electronic circuits. To the best of our knowledge, no studies have been reported on solvent-free fabrication of GoP based in-plane all carbon passive electronic circuits, pH sensor and humidity sensor. Although a GoP temperature sensor has been reported, it's practical applicability as a temperature sensor is unclear with no insight to the performance in terms of repeatability and response/recovery times [14]. In this work we report the dynamic characteristics of temperature sensor by exposing it to candle flame repeatedly. Moreover, being an all-carbon temperature sensor, it doesn't involve the usage of any metal contacts, thereby eliminating the contact resistance losses.

2. Experiments

2.1. Fabrication of sensors and circuits

2.1.1 Fabrication of temperature and pH sensor

A 30 mm x 5 mm rectangular graphite film was deposited on cellulose paper (EW-81051-92, Advantec, USA)by direct writing of HB graphite pencil on paper with the help of scale for several times till required resistance was achieved. As fabricated device was used as both temperature sensing and pH sensing independently.

View Article Online
DOI: 10.1039/C6RA21457F

2.1.2 Fabrication of humidity sensor

An interdigitated electrode capacitor with 12 electrode digits, 2 mm digit width, 1 mm spacing between digits and 20 mm overlapping length was fabricated by direct drawing of 5B graphite pencil on paper with the help of scale. As fabricated device was employed as a humidity sensor.

2.1.3 Fabrication of RC filters

A first order RC filter was fabricated by direct writing of 4 mm x 1.5 mm horizontal HB graphite trace on paper in series with an interdigitated capacitor with 12 digits, 1 mm digit width, 1 mm separation between digits and 20 mm overlap length of digits was drawn by 5B graphite pencil on paper. As fabricated device was utilized as integrator and differentiator.

2.2 Characterization of sensors and circuits

Field Emission Scanning Electron Microscopy (FESEM, supra 40, Carl Zeiss AG) was used to study the surface morphology of the cellulose paper and graphite trace on paper. Senterra Invia Raman Spectrometer (Senterra, Bruker, UK) with 532 nm laser excitation and 10 mW/cm^2 optical power was used for Raman characterization of graphite on paper. The resistance of the pH sensor with different pH solutions was measured using Arduino Uno development board by connecting the device in Arduino ohm meter configuration. The capacitance of the humidity sensor was measured using Arduino Uno by connecting the device in Arduino capacitance meter configuration. Temperature-dependent electrical characterization was performed using Pheonix PM8, Kaurl Suss to measure the resistance of temperature sensor from 29 ^{0}C to 120 ^{0}C in steps of 5 ^{0}C. The electrical properties (sinusoidal

View Article Online
DOI: 10.1039/C6RA21457F

and square wave response) of the low pass and high pass RC circuits were measured by using a digital storage oscilloscope DSO3062a, Agilent.

3. Results and Discussions

Pencil graphite is a composition of graphite, clay and wax. The abrasion of pencil on paper leaves chunks of conductive graphite flakes which range from mono to few layers graphene. Figure 1(a) and 1(b) demonstrate the direct writing of pencil on paper to deposit graphite flakes. The writing of pencil on paper is repeated for several times to achieve required

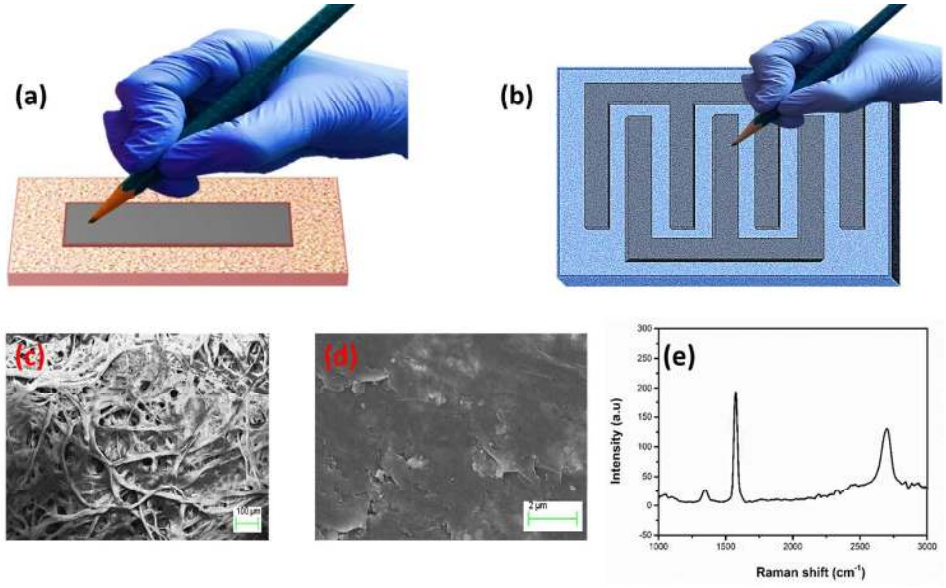

Figure 1: (a),(b) Schematic representation of fabrication of graphite on paper resistive and interdigitated capacitive sensors; (c) SEM image of cellulose paper; (d) SEM image of graphite on paper; (e) Raman spectra of HB pencil graphite.

conductivity. Since different pencils have different compositions of graphite, clay and wax [17], they exhibit different conductivities for similar length, width and thickness of the pencil graphite deposition. The hard pencils (H series) are less conductive compared to those of soft

View Article Online
DOI: 10.1039/C6RA21457F

pencils (B series) as graphite content in hard pencil is relatively less compared to that of soft pencils. Hard pencils were used to draw high resistance traces and soft pencils were used to design low resistance interdigitated lines to implement resistors and capacitors on paper. Field emission scanning electron microscopy (FESEM) was used to study the surface morphology of the paper and pencil graphite deposition on paper. Figure 1(c) indicates that the paper contains a fiber network and it has porous structure. The rough surface of the paper ensures the deposition of graphite flakes ranging from few layers of graphene to multi layers of graphene during the writing of pencil on paper and is continuous as depicted in figure 1(d). (See figure S1, Supplementary Information for more SEM images showing morphology of graphite on paper at different magnification levels). Raman spectroscopy was used to analyze the defect quantity in HB pencil graphite. The Raman spectra of HB pencil graphite shown in figure 1(e) shows two main peaks at wave numbers 1350 and 1580 corresponding D and G peaks which represents the level of defects and sp^2 bonded carbon networks inside graphite respectively.

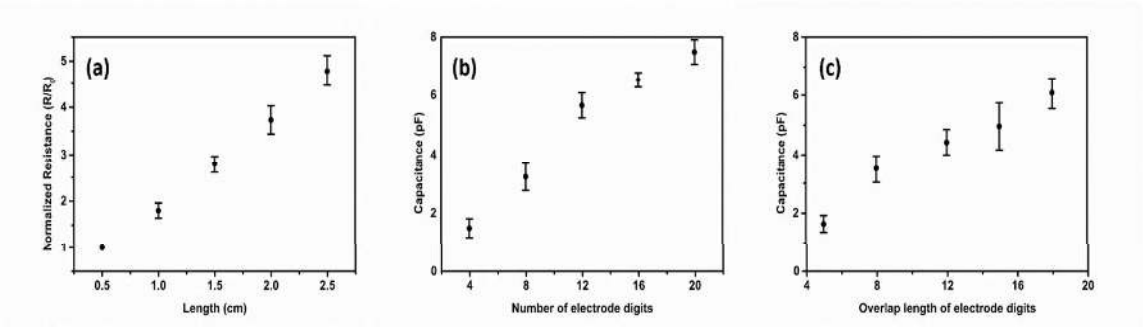

Figure 2: (a) Normalized resistance with the length of the trace (N=3); (b) Capacitance of interdigitated capacitor with the number of electrode digits (N=5); (c) Capacitance of interdigitated capacitor with the overlap length of electrode digits (N=5)

In order to study the variation of resistance with the variation in length of the pencil trace the normalized resistance of HB pencil trace was measured by keeping the width of the trace constant at 5mm and plotted as shown in figure 2(a). The normalized resistance increases with increase in length

View Article Online
DOI: 10.1039/C6RA21457F

of the trace and this variation is almost linear with respect to the length of the trace. Similarly, the properties of 5B pencil interdigitated capacitor on paper was studied by measuring the capacitance of the device with variation in either the number of interdigitated lines or overlapping length of digits by keeping other parameter constant as shown in figure 2(b) and 2(c). It was observed that the capacitance increases with increase in overlap length and number of digits, which is attributed to the increase in overlapping area of interdigitated lines and is consistent with the interdigitated capacitor properties reported with silver ink printed on paper [7]. The large variation in resistance and capacitance in figure 2 can be attributed to the imperfections in making the device, non-uniformity of graphite film on paper.

3.1 Temperature sensor

A 30 mm x 5 mm HB pencil trace on paper is employed as a temperature sensor. The resistance of the sensor was measured by increasing the tempearture in steps of 5 ^{0}C from room temperature (29 ^{0}C) to 120 ^{0}C. Figure 3(a) shows the average and standard deviation of variation in the resistance of 3 GoP devices as a function of temperature. It can be seen that the average resistance of the trace decreased by 38% with an increase in temperature from 29 ^{0}C to 120 ^{0}C. The decrease in resistance of pencil graphite trace with increase in temperature indicates the semiconducting nature of graphite. This thermally activated conduction in graphite trace on paper can be explained as follows:

The resistance in graphite film is due to (i) graphite grain resistance and (ii) grain boundary resistance [18,19]. From Raman spectra, it can be observed that the defects in pencil graphite are large in number and thus the free carriers trapped at grain boundaries, creating a potential barrier which hinders the motion of carriers across the grains. Therefore the resistance due to grain boundaries is large and predominant compared to resistance due to grains. This grain boundary resistance can be represented by eq (1)

View Article Online
DOI: 10.1039/C6RA21457F

$$R \sim R_0 \exp\left(\frac{\Phi}{kT}\right) \qquad (1)$$

where k is Boltzmann's constant and Φ is the potential barrier height. The variation in resistance with temperature can be linearly expressed by using Arrhenius equation:

$$\ln\left(\frac{R}{R_0}\right) = \frac{\Phi}{kT} + c \qquad (2)$$

where c= $-\frac{\Phi}{kT}$ and R_0 is the resistance of the trace at temperature T_0. The potential barrier height was found to be 50 meV from the slope Arrhenius plot shown in figure 3(b), which is comparable to the activation energy of MWCNT trace on paper [8]. The motion of the carriers across the potential barrier can be due to tunneling and thermionic emission. As the potential barrier height is very low, thermionic emission is dominant and is primarily responsible for decrease in resistance of graphite trace on paper with increase in temperature [14]. It can be observed that there exists a significant deviation in response of temperature sensor above 80 ^{0}C in figure 3(a) and non-linearity in Arrhenius plot in figure 3(b) which can be attributed to variation in thickness of graphite film on paper [38]. Controlling the thickness of graphite film by direct writing is a challenge and this standard deviation can be reduced if the thickness of the samples is approximately same. The thickness of graphite can be measured and controlled using Atomic Force Microscopy (AFM) or Transmission Electron Microscopy (TEM) or Profilometer.

View Article Online
DOI: 10.1039/C6RA21457F

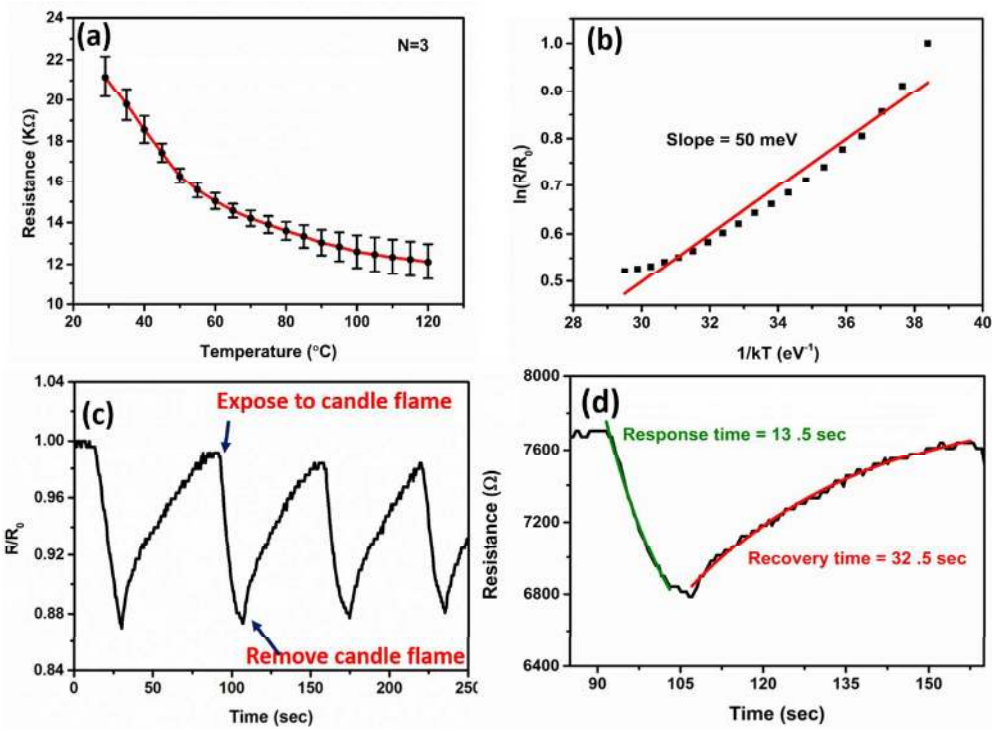

Figure 3 (a) Resistance of temperature sensor as a function of temperature; (b) Arrhenius plot of temperature sensor; (c) temporal response of temperature sensor with candle flame; (d) Exponential fitting of response of temperature sensor under flame test.

The variation in resistance is then quantitatively measured using temperature coefficient of resistance (TCR), which is a figure of merit of a temperature sensor.

$$TCR = \frac{1}{\Delta T}\frac{\Delta R}{R} = \frac{1}{R(T_0)}\frac{R(T)-R(T_0)}{T-T_0} = \frac{-E_a}{kT^2} \qquad (3)$$

where $R(T_0)$ and R(T) are resistances at temperatures at T0 and T respectively. The measured TCR value is -4232 ppm/K or -0.004232 / ^{0}C, which is comparable to the existing standard temperature sensors such as nickel, copper and platinum [20]. This TCR value is comparable to temperature sensor reported with MWCNT on paper [8], reduced graphene oxide based temperature sensor [21] and one order larger than solution processed MWCNT based temperature sensors [22]. Large TCR values of GoP sensor can be attributed to large number of defects present in pencil graphite. This value of TCR indicates that graphite on paper can be used as temperature sensors such as thermistors, anemometers and IR bolometers. As the

View Article Online
DOI: 10.1039/C6RA21457F

ignition temperature of paper is well above 200 ^{0}C, it can be used over a wide range of temperatures from 25 ^{0}C to 150 ^{0}C.

The dynamic characteristics of GoP temperature sensor was investigated by exposing it to a candle flame. The temporal normalized resistance of the sensor was measured by exposing it to the flame for 15 sec and allowed to recover repeatedly as shown in figure 3(c). The response of the sensor to flame and its recovery to initial resistance is exponential function of time as shown in figure 3(d). The response time of the sensor, time taken to reach 90% of its final value is 10 sec and the recovery time of the sensor is 41 sec. The response time is comparable to that of standard platinum temperature sensor Pt 111 (Response time: 8.66 sec, Recovery time: 15.51 sec) [21], recently reported silver ink on paper based temperature sensor [23] and one order faster compared to that of organic compound based temperature sensor [24] whereas the recovery time is comparable to the later.

3.2 pH sensor

A 30 mm X 5mm trace of HB pencil graphite on paper is used as a pH sensor. The pencil graphite trace contains a small fraction of oxygen rich C-O/C-OH and carboxyl groups and Hard (H series) and HB pencil contain more oxygen content compared to the soft pencils (B series) [15,16]. The oxygen functional groups make the graphite film on paper p-type semiconductor and hence the holes are majority carriers. Upon exposure to acidic solutions, the H^+ ions accept electrons from π-orbital of graphite, which results in increase in majority carrier concentration, thereby increasing the electrical conductivity. In contrast, when graphite is exposed to alkaline solutions, OH^- ions donates electrons to π-orbital of graphite thereby causing a reduction in electrical conductivity [26]. Hence H^+ and OH^- ions concentrations affect the generation of holes and electrons in graphite resulting in variation in

View Article Online
DOI: 10.1039/C6RA21457F

resistance of graphite. Moreover, the oxygen functional groups present in graphite undergoes protonation in presence of H^+ ions and thus majority carriers increases which leads to increase in conductivity [25] as shown in figure 4. In contrast, the oxygen groups undergo deprotonation in presence of OH^- ions leading to decrease in majority carriers and hence results in a decrease in conductivity. Thus the conductivity of pencil graphite decreases with increase in pH.

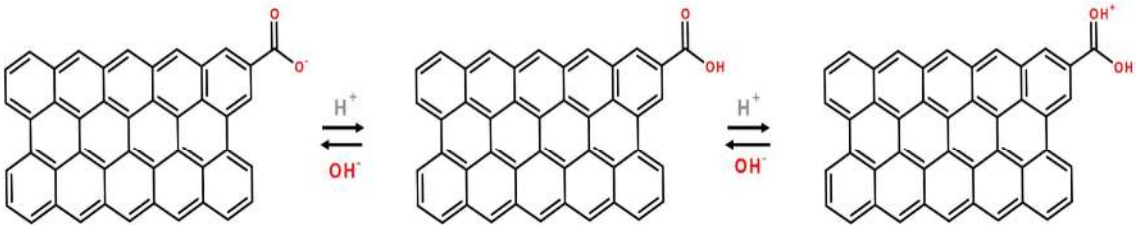

Figure 4: Protonation and de-protonation of oxygen functional groups present in pencil graphite in presence of H^+ and OH^- ions.

In order to evaluate the performance of pH sensor, the variation in resistance of the sensor was measured by drop casting lemon juice (pH=3.5), detergent solution (pH=10) and DI water (pH=7). Being a paper based sensor, it absorbs liquid upon exposure to a pH solution and cannot be reused. As the sensor is meant for one time use 9 similar disposable sensors with small deviation in base resistance were made for sensing pH. 20 µL of each pH solution is drop cast on 3 devices each and normalized change in the resistance of the each sensor was measured upon exposure to acidic, alkaline and neutral solution. The variation in normalized resistance of the sensor with time upon exposure to different pH solutions is as illustrated in figure 5(a) (The individual response of 9 devices to pH is included in figure S2, Supplementary Information). It can be seen that the variation in resistance increased with increase in pH value and it is in accordance with the behavior reported in oxygen rich carbon based pH sensors [25, 26].

View Article Online
DOI: 10.1039/C6RA21457F

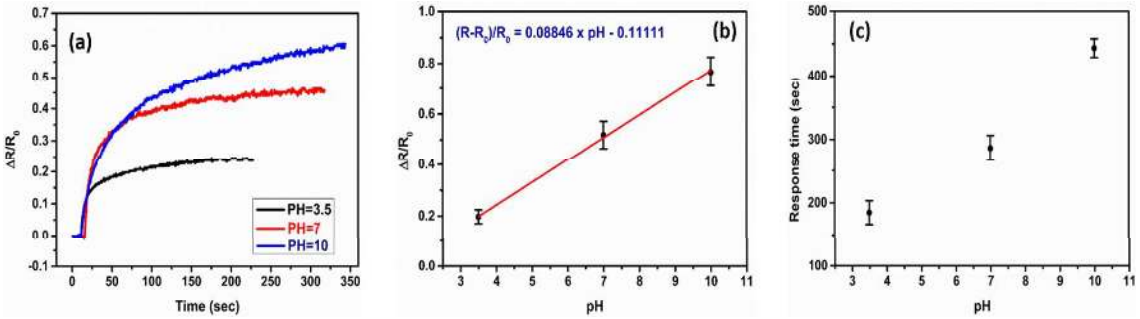

Figure 5: (a) Temporal response of pH sensor with 3 different pH solutions; (b) Normalized change in resistance of pH sensor as a function of pH (N=3 devices); (c) average response time of 3 pH sensors as a function of pH.

The average and standard deviation of relative change in resistance of 3 devices for each pH solution were measured for comparison and plotted as shown in figure 5(b). The response of the pH sensor with different pH solutions is linear and can be expressed as

$$\Delta R/R_0 = 0.08846 \text{ x pH} - 0.13545$$

where R is the initial resistance and ΔR is the change in resistance of the graphite trace on paper after drop casting pH solution. The sensitivity is determined by $0.08846R_0$. We used an average base resistance from 20 kΩ to 25 kΩ throughout the experiment. Therefore the sensitivity of the pH sensor lies in the range of 1.77 kΩ/pH to 2.21 kΩ/pH, which is very high compared to the graphene on paper based pH sensor reported in the literature [27]. The high sensitivity of GoP pH sensor is attributed to the oxygen functional groups present in pencil graphite. Further we calculated the response time, the time taken to reach final and stable resistance value, of 3 devices for each pH solution and their average is plotted as shown in figure 5(c). The response time varies with the pH of the solution and it can be seen that the average response time increases with increase in pH value, which can be attributed to interaction speed between hydrogen ions and graphite [26]. Pristine carbon materials are equally sensitive to both the metal ions and pH and this sensitivity is nominal. However, the oxygen functional groups present in pencil graphite are sensitive to pH and insensitive to

View Article Online
DOI: 10.1039/C6RA21457F

metal ions and this sensitivity towards pH is larger compared to that of pristine materials [25]. Therefore the cross sensitivity of proposed pH sensor to metal ions is very low and is negligible. The reported GoP pH sensor is a low cost, disposable and eco-friendly sensor that can find applications in numerous fields. It can be used to identify the type (acid or alkaline) of solution by measuring the change in resistance relative to the resistance in neutralized water. Therefore it allows to recognize the hazardous solutions in crucial situations when pH test strips are not available readily and in paper based disposable microfluidic applications.

3.3 Humidity Sensor

A 5B pencil graphite on paper interdigitated capacitor with 12 digits (n), 2 mm digit width (w), 1 mm spacing between digits (d) and 20 mm overlapping length (l) of digits is utilized as a humidity sensor. 5B pencil was preferred over HB pencil as conductivity of 5B pencil is superior to that of HB pencil which makes the interdigitated electrodes more conductive in the former case. Cellulose paper contains cellulose fiber networks and these fibers are composed of glucose molecules attached to each other to form a cellulose chain and contains polar OH groups. The individual cellulose fibers are connected to each other with weak intermolecular hydrogen bonding between polar OH molecules of adjacent cellulose fibers. When the cellulose paper comes in contact with moisture, the water molecules participate in weak intermolecular hydrogen bonding with Polar OH groups as demonstrated in figure 6, and penetrate between the cellulose fibers thereby increasing the dielectric constant of the material.

View Article Online
DOI: 10.1039/C6RA21457F

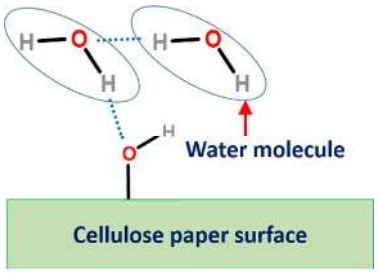

Figure 6: Adsorption of water molecules on cellulose paper surface and formation of weak intermolecular hydrogen bonding.

The porosity of cellulose paper is responsible for absorption and evaporation of moisture relative to humidity levels. Due to the tendency of paper to adsorb moisture from air, the number of water molecules adsorbed to the hydroxyl groups on cellulose paper increases with increase in humidity levels and thus the dielectric constant of the sensor varies. The capacitance of the sensor is given by

$$C = (n-1)\, \varepsilon_r\, \varepsilon_0\, A/d$$

where A is the overlapping area between two digits, ε_r is the relative permittivity of the dielectric medium between two finger digits of interdigitated sensor, ε_0 is the permittivity of free space and d is the distance between two conductive digits in the sensor. As water has a relative permittivity of > 80 at room temperature, which is very high compared to that of paper, the capacitance increases with increase in humidity levels.

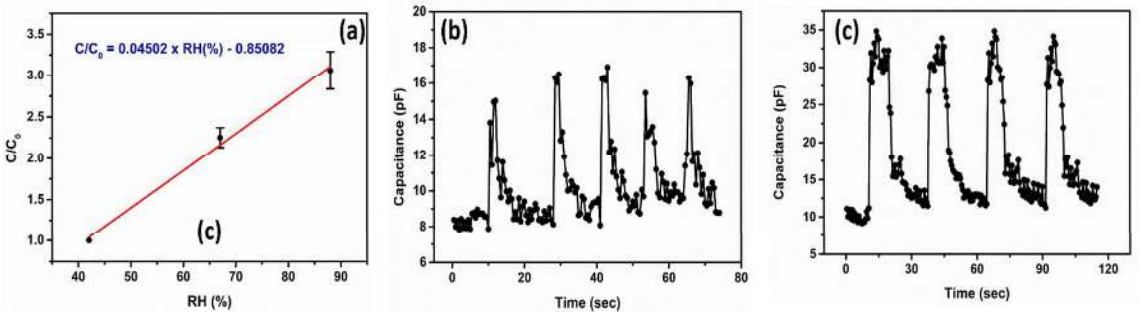

Figure 7: (a) Normalized capacitance of humidity sensor as a function of relative humidity (%RH) (N=3devices); (b) temporal response of humidity sensor with exhaled human breath; (c) temporal response of humidity sensor with water vapor.

View Article Online
DOI: 10.1039/C6RA21457F

The performance of humidity sensor was investigated by exposing it to 3 different relative humidity (RH) levels: room temperature (42% RH), human breath (67% RH) and water vapor (88% RH). These humidity levels were measured using commercially available humidity sensor. The average and standard deviation of normalized capacitance as a function of percentage relative humidity of 3 devices were calculated and plotted as shown in figure 7(a). It was observed that the capacitance of the sensor increases almost linearly with increase in relative humidity levels, which is in agreement with mechanism explained in the previous section. The sensor exhibited a sensitivity of 4.5%/%RH and is comparable to expensive and solvent processed carboxyl CNT on paper and silver ink on paper humidity sensors [23, 34]. Further we investigated the dynamic response of the sensor by exposing it to exhaled breath and water vapor repeatedly. Figures 7(b) and 7(c) show consistent and repeatable response to breath and water vapor respectively. The response and recovery time of the sensor are 2 sec and 7 sec for exhaled breath and 1.5 sec and 6 sec for water vapor. The response and recovery times of GoP humidity sensor reported in this work are one order faster than that of humidity sensors fabricated using conventional eco-unfriendly fabrication procedures, sophisticated and energy consuming equipment and expensive and toxic materials [28-30]. These fast response and recovery times of the sensor are due to faster adsorption and de-adsorption times of water drop on paper. The faster adsorption is due to the capillary pressure and the higher permeability of the cellulose paper [31]. The evaporation rate depends on the mass change during evaporation which is directly proportional to the radius of water droplet. The water droplet on porous cellulose paper surface is larger compared to non-porous surfaces because of spreading which leads to faster evaporation [32]. The performance and properties of this humidity sensor is compared with the other humidity sensors reported on various rigid, plastic and paper substrates as shown in Table 1. Being a

View Article Online
DOI: 10.1039/C6RA21457F

solvent-free and low cost approach, this can be utilized in developing disposable atmospheric humidity sensors.

Table 1: Comparison of fabricated GoP based humidity sensor with reported literature

Sensing platform	*Sensitivity*	*Response & Recovery times (sec)*	*Is it biodegradable?*	*Is it solvent-free process?*	*Fabrication Complexity & Cost*	*Ref.*
Silver interdigitated electrodes on Polyimide (PI)	5.537 pF / %RH	20-109.4 & 21.9-47.7	No	No	Simple & Low cost	28
Silver interdigitated electrodes on Poly amic acid (PAA)	0.185 pF/%RH	41.2-230.4 & 34.6-100.2	No	No	Simple & Low cost	28
CMOS parallel plate capacitive sensor	0.566 % / % RH	6 & NA	No	No	Complex process & relatively expensive	29
MEMS based sensor	2.83 kΩ / %RH	10 & 5	No	Yes	Complex fabrication process & relatively expensive	30
Graphene Oxide (GO) based sensor	NA	0.02-0.03 & 0.03-0.09	No	No	Simple & low cost	33
Multi-walled Carbon Nanotubes (MWCNT) on paper	6% /%RH	6 & 120	Yes	Yes	Simple & expensive	34
Silver interdigitated electrodes on paper	0.18%/%RH	1.2-2 & 1.33-3.2	No	No	Simple & low cost	23
Pencil drawn graphite interdigitated electrodes on paper	4.5%/%RH	1.5-2 & 6-7	Yes	Yes	Simple and relatively cheaper	This work

View Article Online
DOI: 10.1039/C6RA21457F

3.4 Passive RC filters

In order to explore the possibility of GoP electronic circuits, the pencil trace in series with interdigitated capacitor is exploited as a first order passive RC circuit as shown in figure 8(a). The pencil trace acts as a resistor and was drawn with HB pencil to get high resistance line. 5B pencil contains more graphite (82%) compared to that of H series, HB series and other lower series B pencils and is more conductive and thus was used to draw the interdigitated capacitor. The resistance of the HB trace was found to be 1.2 MΩ. To study the functionality of RC filter as an integrator, a square wave input was applied across series RC circuit using a function generator and the output across the capacitor was measured using a digital storage oscilloscope as shown in figure 8(b). At lower frequencies, the output of the filter is almost similar to the input with reduced amplitude as depicted in figure 8(c). As frequency increases the rise time of the waveform increases and finally the waveform becomes triangular in shape with further increase in frequency as shown in figures 8(d) and 8(e). This change in shape of the output of waveform is attributed to the variation of reactance X_c with the variation of frequency of the input signal as given by the following equation

$$X_c = {}^{1}\!\Big/\!_{2\pi f(C + C_p)}$$

where f is the frequency of the input signal, C is the capacitance of the interdigitated capacitor and C_p is the capacitance of the oscilloscope probe (15 pF). The output voltage across the capacitor can be determined by

$$V_{out} = V_{in} \; {}^{X_c}\!\Big/\!_{(R^2 + {X_c}^2)^{\frac{1}{2}}}$$

View Article Online
DOI: 10.1039/C6RA21457F

As frequency increases, the reactance decreases so that the output voltage across the capacitor decreases. The frequency at which the gain falls by 3 dB is the cut-off frequency of the filter and is found to be 6 KHz as shown in figure 8(f). The capacitance of the interdigitated capacitor was found to be 6 pF by using the relation

$$f_c = {}^{1}\!/_{2\pi R(C + C_p)}$$

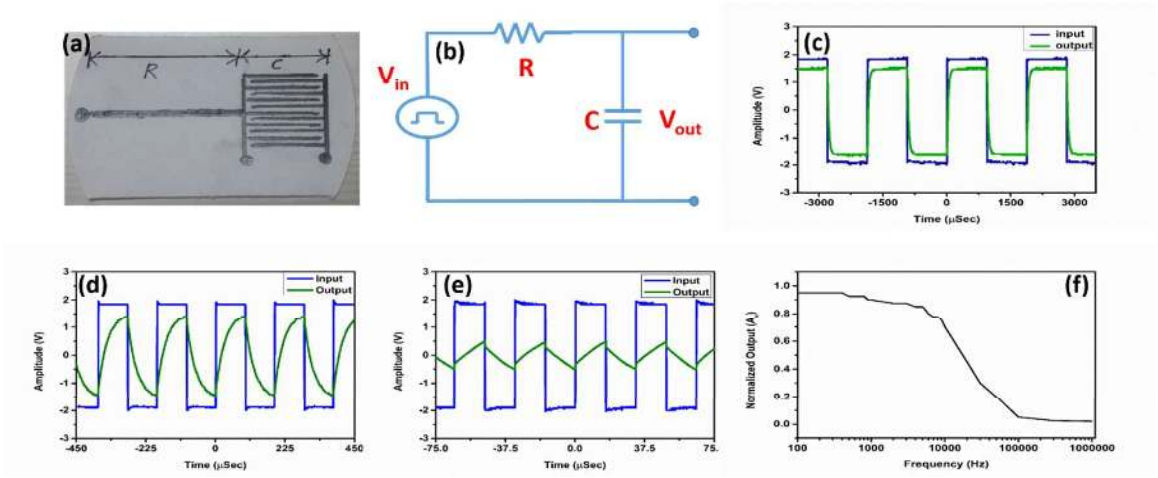

Figure 8: (a) Pencil drawn RC circuit on paper; (b) Schematic of RC integrator circuit ; Low pass filter (Integrator) input (blue) and output (green) at (c) 500 Hz, (d)5 kHz and (e) 30 kHz; (f) Normalized output vs frequency of low pass filter.

Similarly, the performance of all-carbon paper based differentiator was studied by applying square wave input across the series RC circuit and measuring the output voltage across the resistor. The differentiator converts the low frequency square wave to spikes and the output resembles the input as frequency increases as shown in figure S3, Supplementary Information, which is in agreement with conventional resistor and capacitor based passive high pass filters.

To further investigate the frequency response of the RC low pass filter with sinusoidal signals, the sine wave input was applied across the resistor from the function generator and the output across the capacitor was observed in the oscilloscope. At low frequencies the low

View Article Online
DOI: 10.1039/C6RA21457F

pass filter allows the signal to pass through with negligible attenuation as shown in figure S4(a), Supplementary Information. As the frequency increases the attenuation increases and the output signal becomes negligible at very high frequencies as observed in figure S4(b) and figure S4(c), Supplementary Information, respectively. Similarly the high pass filter allows the signal to pass through the circuit with small attenuation at higher frequencies and significantly attenuates the signal at low frequencies as shown in figure S5, Supplementary Information.

Table 2: Comparison of Graphite on paper (GoP) based RC filters

Materials	*Cut-off frequency (f_c)*	*Is it biodegradable?*	*Is it solvent-free process?*	*Is it planar?*	*cost*	*Reference*
Pencil graphite and Ion gel	9 kHz	Partially	No	Yes	Low	10
Pencil graphite and NaCl salt	9 kHz	Yes	No	No	Low	11
Only Pencil graphite	6 kHz	Yes	Yes	Yes	Very Low	This work

The successful fabrication of passive electrical components and their combinational circuits by direct writing of pencil trace on cellulose paper suggests that simple and complex passive RC circuits can be implemented with desired resistance and capacitance by varying the physical dimensions of the pencil trace on paper. Moreover, this is a solvent-free and eco-friendly approach to fabricate biodegradable planar electronic circuits on paper as opposed to the fabrication of electronic circuits on paper reported in literature as shown in Table 2.

3.5 Effect of thickness of graphite film on paper on sensitivity of the sensors

View Article Online
DOI: 10.1039/C6RA21457F

The thickness and uniformity of the graphite film affect the sensitivity of the sensors as explained below

pH sensor: Pure graphite is hydrophobic but pencil graphite has some oxygen rich functional groups which makes it somewhat hydrophilic. However, the hydrophobicity increases with increase in thickness of multilayered graphene or graphite film [41]. It reduces the efficiency of graphite to absorb a liquid. Thus the relative change in conductivity of thick material upon exposure to a acidic or alkaline solution is less compared to that of thin films. Hence the sensitivity of pH sensor decreases with increase in thickness of the graphite film.

Temperature sensor: Graphite has multiple interlayers that are sandwiched between two surface layers. The effect of temperature on thermal motion velocity of surface electrons is negligible. However the thermal velocity of interlayer channel electrons is significantly affected by the temperature and this effect is more when the thickness of graphite is increased. Thus the variation in conductivity with variation in temperature increases with increase in thickness of the graphite film. Therefore the thicker films have higher TCR compared to thin films [38].

Humidity sensor: The capacitance of the sensor depends on the thickness of the electrodes as given by the equation below [39, 40].

$$C = C_1 + C_2 + C_3$$

where $C_1 + C_3 = \varepsilon_0 \left(\frac{\varepsilon_1+\varepsilon_3}{2}\right) \frac{K\left(\sqrt{1-x^2}\right)}{K(x)}$

View Article Online
DOI: 10.1039/C6RA21457F

$$C_2 = \varepsilon_0 \varepsilon_2 \, t/d$$

Here k(x) is a characteristic parameter that depends on geometry of the interdigitated capacitor, $\varepsilon_0, \varepsilon_1, \varepsilon_2$ and ε_3 are dielectric constants of free space, air, medium between electrodes and the substrate and t is the thickness of electrodes. In this case $\varepsilon_1 = \varepsilon_2$ as medium between electrodes is air. As the thickness t increases the capacitance C_2 and hence the total capacitance C increases. Thus the initial capacitance of thicker electrodes is more compared to that of thin electrodes. However, the humidity affects the capacitance only due to substrate (C_3) and this variation in capacitance is constant irrespective of thickness of electrodes. It is well known that a fixed variation in small quantity is more observable compared to that of large quantity. Therefore the sensitivity of humidity sensor will decrease with increase in thickness of the graphite film on paper.

Uniformity of the graphite film on paper is necessary to reproduce the sensors with sensitivity with least device to device variation. However, porous nature of cellulose paper makes it difficult to get uniform film on paper and there will be a measurable variation or deviation in sensitivity from device to device. However, this method being low cost and eco-friendly is beneficial for small scale production where cost and environment are major concerns at the expense of deviation in accuracy. This report is a proof of concept of direct writing of graphite on paper to make low cost and eco-friendly paper electronics and chemical sensors that can be applied in numerous fields and as authors, we are optimistic that realizing the tremendous potential this strategy has, there will be significant interest in this area which will lead to a need to find tools that can write electronics on paper with greater precision and uniformity suitable for commercialization.

View Article Online
DOI: 10.1039/C6RA21457F

So far, numerous electronic circuits, physical and chemical sensors have been reported on plastic substrates like Polyimide (PI) and Polyethylene terephthalate (PET). Despite the excellent performance of these devices, non-biodegradability restricts their use to limited applications [13] and PET substrate cannot be used above 110 ^{0}C [35]. Alternatively, paper is biodegradable and can be processed up to 200 ^{0}C. However, the existing fabrication strategies utilize either expensive materials, equipment or toxic solvents, which make paper electronics expensive and eco-unfriendly. Here we report the alternative low cost, eco-friendly and solvent-free fabrication method to develop electronic circuits and sensors by direct drawing of pencil trace on paper. The estimated cost of the each device is < \$0.1. Such proposed technology will significantly reduce the electronic-waste generated due to the non-recyclable and non-biodegradable electronics which is a major problem worldwide leading to significant health issues and environment contamination [36, 37].

Conclusion

In summary, graphite on paper was used as a functional material to implement electronic components such as resistors, capacitors, their combinational first order passive circuits and physical and chemical sensors such as temperature sensor, pH sensor and humidity sensor. This was achieved via direct writing or mechanical abrasion of graphite pencil on cellulose paper which involves the deposition of few layers to multi layers of conductive graphene flakes intercalated by clay and wax. The performance of the as fabricated devices was similar to those fabricated by using capital intensive equipment and eco-unfriendly materials. This approach offers a simple, solvent-free, eco-friendly, inexpensive green fabrication method of passive electronic devices and physiochemical sensors on paper, in use-and-recycle or use-and-throw electronics applications.

View Article Online
DOI: 10.1039/C6RA21457F

Acknowledgement

The authors acknowledge the financial support from **Science and Engineering Research Board (SERB)**, Department of Science & Technology, Government of India, Grant # YSS/2015/000863. SK thanks Harshit Gupta, 2nd year B.Tech student, Department of Electrical Engineering, Indian Institute of Technology Ropar, India, for his assistance in characterization of the sensors using Arduino Uno development board.

References

[1] D. Tobjork and R. Osterbacka, *Adv. Mater*., 2011, 23, 1935-1961.

[2] S. K. Mahadeva, K. Walus and B. Stoeber, *ACS Appl. Mater. Interfaces*, 2015, 7, 8345-8362.

[3] N. Dossi, R. Toniolo, A. Pizzariello, E. Carrilho, E. Piccin, S. Battiston and G. Bontempelli, *Lab Chip*, 2012, 12, 153–158.

[4] N. C. Sekar, S. A. M. Shaegh, S. H. Ng, L. Ge and S. N. Tan, *Sens. Actuators, B*., 2014, 204, 414-420.

[5] F. Pettersson, T. Remonen, D. Adekanye, Y. Zhang, C. E. Wile´n and R. O¨sterbacka, *ChemPhysChem*, 2015, 16, 1286-1294.

[6] Y. Wang, Y. Shi, C.X. Zhao, J.I. Wong, X.W. Sun, H.Y. Yang, *Nanotechnology*, 2014, 25, 094010.

[7] R. Z. Li, A. M. Hu and T. Zhang, *ACS Appl. Mater. Interfaces*, 2014, 6, 21721-21729.

[8] S. Kanaparthi and S. Badhulika, *Nanotechnology*, 2016, 27, 095206.

[9] K.M. Frazier, K. a Mirica, J.J. Walish and T.M. Swager, *Lab Chip*., 2014, 14, 4059-66.

[10] N. Kurra, D. Dutta and G. U. Kulkarni, *Phys. Chem. Chem. Phys*., 2013, 15, 8367-8372.

[11] P. Nath, I. Hussain, S. Dutta and A. Choudhury, *Indian J. Phys.*, 2014, 88, 1093-1097.

View Article Online
DOI: 10.1039/C6RA21457F

[12] G. Zheng, L. Hu, H. Wu, X. Xie and Y. Cui, *Energy Environ. Sci*., 2011, 4, 3368-3373.

[13] S. Kanaparthi and S. Badhulika, *Green Chem*., 2016, 18, 3640-3646.

[14] T. Dinh, H. P. Phan, D. V. Dao, P. Woodfield, A. Qamar and N. T. Nguyen, *J. Mater. Chem. C*, 2015, 3, 8776-8779.

[15] C. W. Foster, D. A. Brownson, A. P. R. de Souza, E. Bernalte, J. Iniesta, M. Bertotti and C. E. Banks, *Analyst*, 2016, **141**, 4055-4064.

[16] C. W. Lin, Z. Zhao, J. Kim and J. Huang, *Sci. Rep*., 2014, 4, 3812.

[17] M. C. Sousa and J. W. Buchanan, *Comput. Graph. Forum*, 2000, 19, 27-49.

[18] T. R. Albrecht, H. A. Mizes, J. Nogami, S. I. Park and C. F. Quate, *Appl. Phys. Lett*., 1988, 52, 362-364.

[19] Y. Gan, W. Chu and L. Qiao, *Surf. Sci*., 2003, 539, 120-128.

[20] J. T. W. Kuo, L. Yu and E. Meng, *Micromachines*, 2012, 3, 550-573.

[21] A. Di Bartolomeo, M. Sarno, F. Giubileo, C. Altavilla, L. Iemmo, S. Piano, F. Bobba, M. Longobardi, A. Scarfato, D. Sannino, A. M. Cucolo and P. Ciambelli, *J. Appl. Phys*., 2009, 105, 064518.

[22] S. Sahoo, S. K. Barik, G. L. Sharma, G. Khurana, J. F. Scott and R. S. Katiyar, ArXiv e-prints, 2012.

[23] J. M. Nassar, M. D. Cordero, A. T. Kutbee, M. A. Karimi, G. A. T. Sevilla, A. M. Hussain, A. Shamim and M. M. Hussain, *Adv. Mater. Technol*., 2016, 1, 1600004.

[24] S. M. Abdullah, Z. Ahmad and K. Sulaiman, K., *Sensors*, 2014, 14, 9878-9888.

[25] P. Gou, N. D. Kraut, I. M. Feigel, H. Bai, G. J. Morgan, Y. Chen, Y. Tang, K. Bocan, J. Stachel, L. Berger, M. Mickle, E. Sejdic and A. Star, *Sci. Rep*., 2014, 4, 4468.

[26] L. Liu, J. Shao, X. Li, Q. Zhao, B. Nie, C. Xu and H. Ding, *Appl. Surf. Sci*., 2016, 386, 405-411.

[27] C. Lee, K. F. Lei, S. Tsai and N. Tsang, *BioChip J*., 2016, 10, 182-188.

View Article Online
DOI: 10.1039/C6RA21457F

[28] T. Yang, Y. Z. Yu, L. S. Zhu, X. Wu, X. H. Wang and J. Zhang, *Sens. Actuators, B,* 2015, 208, 327-333.

[29] V. P. Chung, C. L. Cheng, M. C. Yip and W. Fang, *presented in part of 28th IEEE International Conference on Micro Electro Mechanical Systems (MEMS)*, Estoril, January, 2015.

[30] C. H. Lin, L. M. Fu and C. Y. Lee, *presented in part of 9th IEEE International Conference on Nano/Micro Engineered and Molecular Systems (NEMS),* Hawaii, April, 2014.

[31] D. Shou, L. Ye, J. Fan and K. Fu, *Langmuir*, 2013, 30, 149-155.

[32] R. F. Griffiths and I. D. Roberts, *Atmos. Environ.*, 1999, 33, 3531-3549.

[33] S. Borini, R. White, D. Wei, M. Astley, S. Haque, E. Spigone, N. Harris, J. Kivioja and T. Ryhanen, *ACS Nano*, 2013, 7, 11166-11173.

[34] J.-W. Han, B. Kim, J. Li and M. Meyyappan, *J. Phys. Chem. C*, 2012, 116, 22094-22097.

[35] H. Zhu, Z. Xiao, D. Liu, Y. Li, N. J. Weadock, Z. Fang, J. Huang and L. Hu, *Energy Environ. Sci.*, 2013, 6, 2105-2111.

[36] B. H. Robinson, *Sci. Total Environ*., 2009, 408, 183-191.

[37] S. Pramila, M. H. Fulekar and P. Bhawana, *Res. J. Recent Sci.,* 2012, 1, 86.

[38] X. Y. Fang, X. X. Yu, H. M. Zheng, H. B. Jin, L. Wang and M. S. Cao, *Phys. Lett. A*, 2015, 379, 2245-2251.

[39] H. E. Endres and S. Drost, *Sens. Actuators, B*, 1991, 4, 95-98.

[40] N. Angkawisittpan and T. Manasri, *Meas. Sci. Rev.*, 2012, 12, 8-13.

[41] M. Munz, C. E. Giusca, R. L. Myers-Ward, D. K. Gaskill and O. Kazakova, *ACS nano*, 2015, 9, 8401-8411.

View Article Online
DOI: 10.1039/C6RA21457F

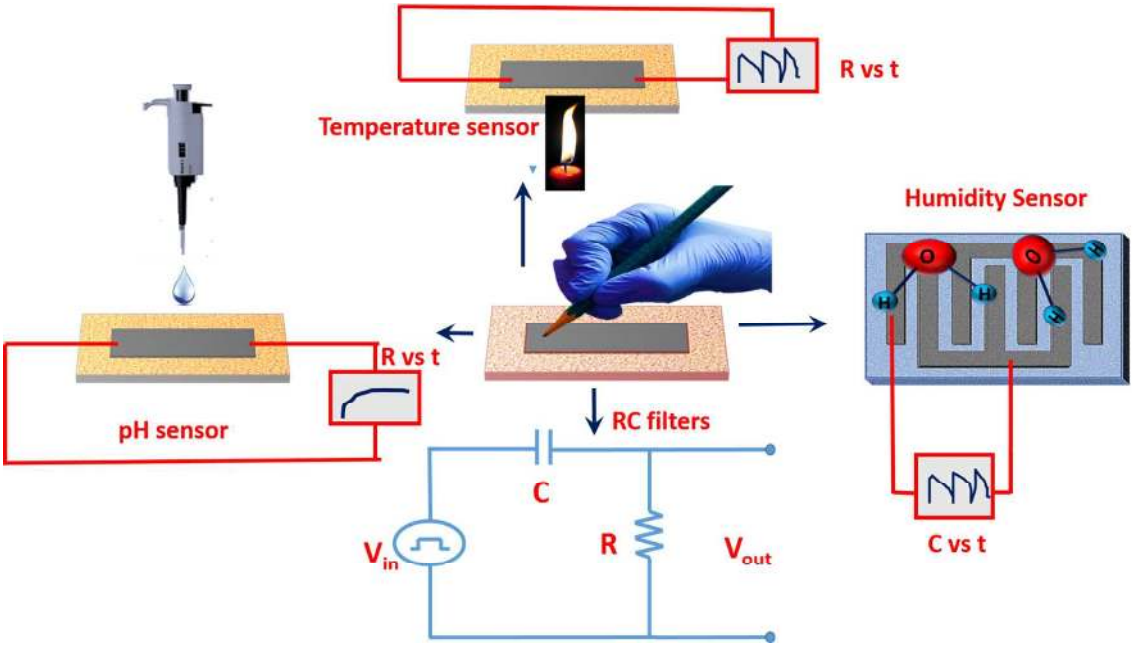

Green fabrication of passive electronic circuits and physiochemical sensors by solvent-free processing of graphite on paper